Magnon vs Phonon effects in electrical transport

Marco Di Gennaro,[1, 2, *] Bin Xu,[3] and Matthieu J. Verstraete[1, 2]
[1] *Department of Physics, Université de Liège, B-4000 Liège, Belgium*
[2] *European Theoretical Spectroscopy Facility (www.etsf.eu)*
[3] *Physics Department and Institute for Nanoscience and Engineering, University of Arkansas, Fayetteville, Arkansas 72701, USA*

We calculate the electron-phonon scattering contribution to spin-dependent transport quantities in ferromagnetic Iron, Nickel and disordered Permalloy solving variationally the semi-classical linearized Boltzmann transport equation. The dynamical matrix is calculated *ab-initio* and the disorder is described within the Virtual Crystal Approximation. We compare our results to the Relaxation Time Approximation which has severe limitations in metals. We find that the resistivity has a characteristic polynomial behaviour according to the magnetic phase, which is easy to derive analytically, while the Seebeck coefficient shows a much more complicated interrelation between different scattering sources. The different scattering mechanisms are not at all independent, which imposes a limitation to Mathiessen's rule. We calculate the spin dependent Seebeck coefficient describing a build up of spin chemical potential under the application of a temperature gradient. We find that a thermal gradient can produce a pure spin current at high temperatures in Permalloy.

Spin-related effects are fundamental topics in solid state physics research [1]. Generation, control and detection of spin accumulation represent important achievements towards revolutionary spintronic technologies [2–6]. Two kinds of spin currents can be generated: those carried by free electrons (or diffusive), which appears only in magnetic metals, and those mediated by magnons, which can also appear in magnetic insulators.
Thermoelectric effects concern the coupling of heat currents and electric currents [7]. Similarly, heat and spin currents can be interrelated in bulk magnetic systems. In this paper, we examine the physics of thermoelectric effects in collinear spin-polarised metals and we calculate spin dependent transport coefficients *ab-initio*. We choose Py since it is widely used as a spin injector in nanomagnetic experiments such as non local spin valves [8, 9] and lateral spin valves [9–13] as well for domain wall motion [14, 15] and has been suggested for applications in spintronic devices [2] due to its advantageous properties such as its low magnetic anisotropy, high Curie temperature (T_C=871 K), and significant spin-dependent scattering that yields a highly spin-polarized current within a few nanometers [16].

The Seebeck effect (SE) is the generation of net electromotive force when a thermal gradient is applied across a material. In the presence of a varying chemical potential μ and a temperature gradient ∇T, the local current density $\mathbf{j}_c$ in a closed circuit is given by: $\mathbf{j}_c = -\sigma\left(\frac{1}{e}\nabla\mu + S\nabla T\right)$, where σ is the electronic conductivity. Two spin counterparts have been discovered for the Seebeck effect (SE), depending on whether the spin current generated from a thermal gradient is a diffusive spin current (known as spin-dependent Seebeck effect or SDSE [10, 17]), or it is rather a magnonic spin current, which goes under the name of spin Seebeck effect (SSE) [18–20]. In spin polarised collinear metals, two spin channels are present. In the absence of spin-flip mechanism these two channels are separated and transport properties are independent for majority and minority spin electrons [21, 22]. Spin dependent current densities read: $\mathbf{j}_{\uparrow,\downarrow} = -\sigma_{\uparrow,\downarrow}\left(\frac{1}{e}\nabla\mu_{\uparrow,\downarrow} + S_{\uparrow,\downarrow}\nabla T\right)$, where we introduce the spin dependent electrical conductivities σ_η and Seebeck coefficients S_η ($\eta = \{\uparrow,\downarrow\}$). The Seebeck coefficient for a ferromagnet is defined as [22]:

$$\langle S\rangle_\sigma = \frac{\sigma_\uparrow S_\uparrow + \sigma_\downarrow S_\downarrow}{\sigma_\uparrow + \sigma_\downarrow}. \quad (1)$$

A diffusive electronic spin current is driven by the SDSE according to [10, 23]: $\mathbf{j}_\uparrow - \mathbf{j}_\downarrow = \mathbf{j}_s = -\sigma_F(1-P^2)\Delta S\frac{\nabla T}{2}$ where $\sigma_F = \sigma_\uparrow + \sigma_\downarrow$, P is the polarization of the conductivity $(\sigma_\uparrow - \sigma_\downarrow)/(\sigma_\uparrow + \sigma_\downarrow)$ and the spin dependent Seebeck coefficient is:

$$\Delta S = S_\uparrow - S_\downarrow \quad (2)$$

The SDSE can be revealed experimentally [8, 10] by using the technique of Non Local Spin Valves (NLSV) [8, 9], which allows to decouple the electrical current from the spin current. The SSE gave input to the so called Spin-Caloritronics [24, 25], and has a more complicated interpretation involving magnon-phonon coupling [18, 26–30]. The main differences between SSE and SDSE can be summarized as i) the characteristic length of the signal (∼1 mm for SSE, ∼1 nm for SDSE) ii) SSE occurs independently of the electronic structure of the material [31, 32], iii) SSE amplitude is of a few nV/K while SDSE is about three orders of magnitude stronger, iv) SSE amplitude scales with the thermal conductivity of the substrate [26], with a high intensity peak at low temperature suggesting strong magnon-phonon coupling. The SSE has therefore a different physical explaination and must be differentiated from SE and SDSE which are the main subjects of this letter.

In the following, we examine the effect of both phonons and magnons (spin disorder) on the electron transport properties, by solving the Boltzmann Transport Equation (BTE) on two levels of approximation: the Relaxation Time Approximation (RTA) model [33] (considering the explicit electron bandstructure) and a fully *ab-initio* Lowest Order Variational approximation (LOVA) [34] in which electron-phonon coupling contribution is taken into account. We show that the resistivity can be fitted well with the RTA model, and electron-magnon scattering is the dominant mechanism below the Curie temperature, and its residual increase above T_c is due to phonons. On the other hand, no single RTA model is able to reproduce the experimental variation of the Seebeck coefficient, and using only phonon scattering returns the same order of magnitude as experimental values, suggesting a partial cancellation of the magnon contribution and a main role of phonons for the diffusive SDSE.

Electrons in real ferromagnetic materials are subject to complex scattering mechanisms. Several interactions have to be considered to correctly describe the deviation from the free electron model: electron-phonon (EP), electron-electron (EE), electron-magnon (EM), disorder, defects, etc. Some of these contributions (disorder, defects) depend on the specific sample characteristics and relatively temperature independent, and are dominant at low temperature. These are absent in the case of pure materials while other contributions (EP,EE,EM,MP) are intrinsic properties. In the hypothesis of two or more independent scattering mechanisms with the same energy dependence [35], the Mathiessen's rule allows to deduce the total mobility from the mobility of the two scattering mechanisms alone. This rule is in practice used for the relaxation time, even though it strictly applies only to mobilities.

A phenomenological estimation of resistivity for spin compensated metals is the Bloch-Grüneisen formula [36–38]: $\rho_{\rm BG} = \rho_0 + \rho(T)$. ρ_0 is called residual resistivity, and is temperature-independent and due to scattering from defects. The temperature dependent part of the resistivity $\rho(T)$ is linear in the temperature for high temperatures while at low temperature usually goes as T^5. Spin-polarized materials present a prevalent quadratic contribution, representing the scattering of itinerant spins at low T by lattice spin waves [39]. At T_c the spin disorder is maximal and so is its contribution to ρ.

A simple analytic expression for the Seebeck coefficient does not exist to our knowledge. For non magnetic materials with "normal" electronic band structures, the Seebeck coefficient has a linear dependence with temperature and the sign of the coefficient gives insight about the nature of the carriers into the material (negative sign for electrons, or n type materials, positive sign in the other case). At low temperatures the phonon-phonon interaction can give rise to phonon-electron drag with a characteristic maximum in $|S|$. If one neglects this effect, Mott derived a simple formula [40]:

$$S = -\frac{\pi^2 k_{\rm B}^2 T}{3e}\left[\frac{1}{\sigma}\frac{d\sigma(\epsilon)}{d\epsilon}\right]_{\epsilon=\epsilon_{\rm F}}, \tag{3}$$

where one can see a ratio between the conductivity and its energy derivative. Any global change in scattering (i.e. non energy dependent) will simplify and leave S unaffected. To change S the scattering must be different for electrons below and above the chemical potential.
When scattering from both phonons and spin-flip interactions are involved, it is difficult to recognise characteristics due to a specific magnetic order, and to disentangle the scattering mechanisms. In particular (see experimental data from the literature below), there is no clear distinction or kink between the ferromagnetic and the paramagnetic phases, as in the case of the resistivity. Electron-magnon drag and phonon-magnon drag also introduce additional low temperature signatures. We will compare progressively more complex models, including either phonons or magnons or both.

Electron and phonon structures, electron-phonon coupling matrix elements and LOVA transport coefficients as implemented in [41] are calculated using the ABINIT package. We consider a collinear spin structure, with two independent spin channels for each material. This is a strong approximation since transport in these systems is also influenced by spin-flip mechanisms [42].
For the RTA approach, the electronic band structures are calculated from density functional theory (DFT), and the transport properties are calculated using the BOLTZTRAP code [43]. Calculation details and a review of the method are given in the SI.

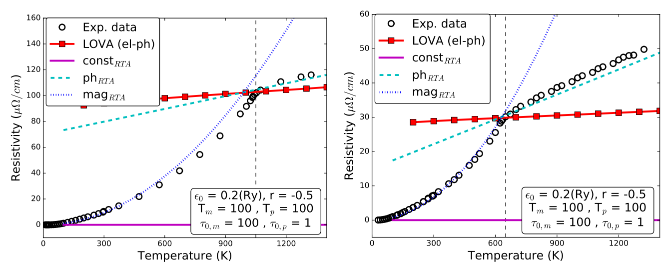

(a) Fe (b) Ni

FIG. 1. Resistivity for Fe (left) and Ni(right). Open black circles: experimental results from Ref. [44]. Red lines with closed squares: LOVA results from electron-phonon interaction. RTA results: constant RTA (purple full lines), RTA with phonon contribution only (cyan dashed line) and RTA magnon contribution only (blue dotted line). Vertical dashed lines correspond to the Curie temperatures.

Resistivity for Fe and Ni are compared to experimental results in Fig. 1. The resistivity for each spin channel is calculated from the electronic structure of the spin channel and the total resistivity is calculated as that of two

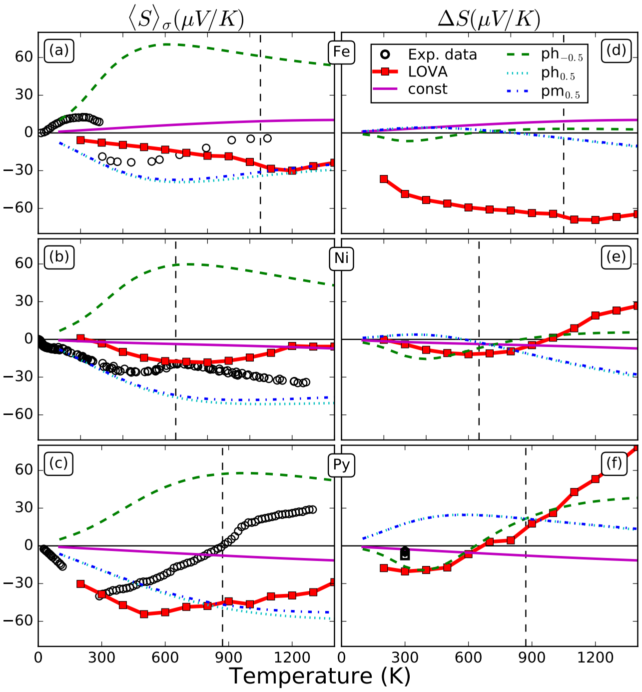

FIG. 2. (Color on line) Top: ferromagnetic Seebeck coefficient $\langle S \rangle_\sigma$, bottom: Spin dependent Seebeck coefficient ΔS. Left: Fe, middle: Ni, right: Py. Black dashed lines with open circles: experimental results from Refs. [18, 44]. Red lines with closed squares: LOVA. Purple lines with top triangles: constant RTA (equal to RTA from magnons only). Dashed lines with open triangles: RTA for phonons only (cyan) and phonon-magnon scattering (blue). Vertical dashed lines denotes Curie temperatures. Open and full triangles refer to RTA with $r = -0.5$ and $r = 0.5$ respectively. Experimental points for ΔS in Py at 300 K: black empty square is from Ref. [8], black empty pentagon and hexagon are from Ref. [10]. The vertical dashed lines represent the Curie temperature of each material.

parallel channels: $\rho_{\mathrm{SP}} = \frac{\rho_\uparrow \rho_\downarrow}{\rho_\uparrow + \rho_\downarrow}$. Black open circles in Fig. 1 represent experimental results from Ref. [44]. Two different phases are clearly distinguishable by the experimental resistivity: a low temperature quadratic and a high temperature linear part. The red solid curves with closed squares represent the LOVA results, while the full-purple, dashed-cyan and dotted-blue curves represent the results from constant RTA (linear), phonon scattering RTA (linear) and magnon scattering RTA (quadratic) respectively. For temperature below the Curie temperature (1043 K for Fe and 628.5 K for Ni), the electron-magnon scattering show good agreement with the experimental data. The RTA parameters are shown in the top-right panel. Both the low temperature ferromangetic quadratic and the high temperature paramagnetic behaviours can be obtained by fitting the RTA model parameters (Tab. 2 in SI).

A quadratic dependence on the temperature was reported also for Py [42, 45]. LOVA resistivity can for the moment be obtained only for phonon scattering (we still miss scattering from spin disorder). The high T slope is roughly correct for Fe and underestimated for Ni, which could be due to thermal expansion or other effects. The high temperature results are shifted along the y axes for simplicity.

All RTA calculations were conducted considering only scattering from acoustic phonons (being the two systems cubic with one atom per unit cell). The parameters used for RTA calculations were fitted on top of Resistivity results and are listed in the panels in Fig. 1.

As already pointed out, there are no well defined temperature dependencies indicating the magnetic order for $\langle S \rangle_\sigma$. We observe nevertheless specific features for $\langle S \rangle_\sigma$: negative sign below T_c with a negative peak and a tendency to zero at T_c. Moreover, $\langle S \rangle_\sigma$ shows a positive maximum at around 200 K for Fe, due to magnon-phonon drag [46], while Nickel presents a slope modification from positive to negative at $T_c = 628.5$ K. For Py the situation is similar to Ni, but $\langle S \rangle_\sigma$ maintains its slope and becomes positive at T_c.

RTA calculations are obtained using the exponent for scattering from acoustic phonons $r = -0.5$ (green dashed lines). We note that with this exponent, it is possible to have neither the correct sign for $\langle S \rangle_\sigma$ nor the minimum in temperature. The value we find that best approximate the experimental results is and the $r = 0.5$ case (scattering from phonons only: dotted cyan lines and scattering from phonons and magnons: dotted-dashed blue lines), which is an average of all scattering effects. A positive exponent for the energy in the phonon lifetime means that the more an electron is close to the Fermi level, the more it will have a high lifetime value, which is in contrast with the parabolic band concept, and a higher mobility close to the Fermi level. This poses some problems which are clearly a limit to the RTA.

The LOVA calculations (red lines with closed squares) give a overall results in agreement with the Seebeck coefficient, which is correct for sign and amplitude, even at low temperature. LOVA returns a result in agreement with a RTA model with a positive (averaged) energy exponent, indicating that contrary to the resistivity, the RTA cannot be used to separate the magnon scattering from the phonon scattering, when the former is present.

Having calculated the Seebeck coefficient for the two spin channels, it is now possible to estimate the SDSE coefficient in Eq. 2. Experimental results for ΔS are rare at the moment, only some recent results from NLSV measurement are available at ambient temperature [8, 10]. The control of the local temperature in the device is also hard to establish, and is usually inferred from finite element simulations. Our methods provides a valuable tool for the estimation of the SDSE coefficient. We predict (Figs. 2 (d, e, f)) that a spin current of several tents of $\mu V/K$ can be generated at elevated temperature, at which $\langle S\rangle_\sigma$ is also minimal, yielding optimal conditions: $\mathbf{j_c} = 0$ and $\mathbf{j_s} = \max$ for spintronics.

Discussion

We use RTA to explore the $\tau(\epsilon)$ dependency plus the effect on $\langle S\rangle_\sigma$. We shift from the perfectly parabolic band structure, considering in its place the *ab-initio* full valence band.

RTA is based on a single band, parabolic model. It works surprisingly well for the resistivity of spin polarized metals, and puts into evidence that two well distinguished phases exists, and in each of the two there is one and only one prevalent scattering mechanism. On the contrary, the RTA totally fails for the Seebeck coefficient when magnons are involved, and this is symptomatic that the scattering events are not disentangleble.

The minimum at intermediate temperature moreover appears for only positive exponents in RTA, meaning that the scattering is energy dependent. A positive r exponent is needed to get the correct sign of $\langle S\rangle_\sigma$ in all cases. This means that scattering from acoustic phonons alone is not enough, which is different from not having phonon scattering at all. On the contrary, we show that taking into account only phonons with a different relaxation time for every electronic band gives the right sign, the right order of magnitude, a minimum below T_c and a decrease in absolute value as the temperature increases. The difference with experimental results can be due to thermal expansion ... RTA also gives extremum in $\langle S\rangle_\sigma$ with a positive r, which therefore is not a band alignment effet. Why $\langle S\rangle_\sigma$ gives an almost zero result close to T_c? Fermi smearing (cRTA) returns neither the minumum with T nor the low value at T_c. Changing r can give the right sign, but we miss information relative to the exchange between bands, as the temperature increases. Most of the $\langle S\rangle_\sigma$ comes from the phonon scattering rather than from a pure electronic structure effect. Moreover, both methods agree that, even if the system is still magnetic and with a higher spin disorder as T_c is approached, the magnon scattering has not a major role in the electron-scattering. Matching experiment gives an estimation of the average exponent.

Missing factor of 2 or so comes from additional effect on the lifetime $\tau(\epsilon)$. Lifetime epsilon dependency goes wrong way to explain magnon induced T^2 dependency: this must come from explicit T dependency of lifetime. This dependency cancels out of the Seebeck formula within the RTA, which explains the weak impact of magnons on the diffusive S. Total S is not just sum of different scattering contributions

We conclude that it does not exists a single r exponent which explains both $\langle S\rangle_\sigma$ and ΔS. Magnons are not the key yo achieve $\langle S\rangle_\sigma$. What is important is to correctly consider phonons.

In conclusion, we calculated spin dependent transport quantities from full ab-initio and mixed model/ab-initio method. We stressed on the role that energy-dependent relaxation time covers and on we found that the inclusion of magnetic scattering imposes the introduction of a new exponent in the RTA, which is the average of all interaction included. On the other side, at the price of a reasonable computation effort, the full ab-initio LOVA calculation allows to take into account EPC from DFPT gives parametrization-free results equivalent to introducing an average energy exponent in the RTA model.

We show that for resistivity the scattering mechanism are easy to distinguish, therefore a RTA model calculation with proper parameters and the full *ab-initio* LOVA are equivalent. The Seebeck coefficient on the contrary needs a physical model difficult to explain (i.e. a positive r exponent), while EPC alone gives a good prediction. The introduction of higher order correction, such as spin flip scattering [47], thermal expansion, and magnon-phonon coupling would improve the numerical agreement.

LOVA results gives a result which is equivalent to the effective electron scattering. For full anaddb calculation there is no single exponent (all phonons present)

The importance of our calculation is that it offers a possibility to calculate the bulk SDSE coefficient which does not depends on the local heating in the experiment. The SDSE shows a complex behaviour, sensitive to the temperature. This is a new possibility to study electronic spin currents in ferromagnetic materials and could help find the most suitable spin current generator at a given temperature.
To the best of our knowledge there are neither SDSE measurements nor calculations for temperatures other than 300 K. We hope this study will stimulate higher temperature work on the SDSE.
Ideally it is possible to project materials which produce no electrical current and non-zero spin current.

We thank B.J. Van Wees and F. Casanova for fruitful discussions. The authors acknowledge an A.R.C. grant (TheMoTherm 10/15-03) and MDG acknowledges a F.R.I.A. grant (number 1.E051.12), both from the Communauté Française de Belgique. Computer time was made available by PRACE-2IP and 3IP on Archer and Hector (EU FP7 grants RI-283493 and RI-312763), CECI, SEGI-ULg and Zenobe

* Email address: marcodigennaro@outlook.com

[1] A. Hoffmann and S. D. Bader, Phys. Rev. Applied **4**, 047001 (2015).

[2] S. S. P. Parkin, M. Hayashi, and L. Thomas, Science **320**, 190 (2008), http://www.sciencemag.org/content/320/5873/190.full.pdf.
[3] J. Katine and E. E. Fullerton, Journal of Magnetism and Magnetic Materials **320**, 1217 (2008).
[4] B. Everitt, D. Olson, T. van Nguyen, N. Amin, T. Pokhil, P. Kolbo, L. Zhong, E. Murdock, A. Pohm, and J. Daughton, Magnetics, IEEE Transactions on **41**, 125 (2005).
[5] G. H. Koh, H. J. Kim, W. C. Jeong, J. H. Oh, J. H. Park, S. Y. Lee, G. T. Jeong, I. J. Hwang, T. W. Kim, J. E. Lee, H. J. Kim, S. O. Park, U. I. Jeong, H. S. Jeong, and K. Kim, *Proceedings of the International Conference on Magnetism (ICM 2003)*, Journal of Magnetism and Magnetic Materials **272–276, Part 3**, 1941 (2004).
[6] I. Žutić, J. Fabian, and S. Das Sarma, Rev. Mod. Phys. **76**, 323 (2004).
[7] M. Zebarjadi, K. Esfarjani, M. S. Dresselhaus, Z. F. Ren, and G. Chen, Energy Environ. Sci. **5**, 5147 (2012).
[8] M. Erekhinsky, F. Casanova, I. K. Schuller, and A. Sharoni, Applied Physics Letters **100**, 212401 (2012).
[9] K. Miura, S. Kasai, K. Kobayashi, and T. Ono, Japanese Journal of Applied Physics **45**, 2888 (2006).
[10] A. Slachter, F. L. Bakker, J.-P. Adam, and B. J. van Wees, Nat Phys **6**, 879 (2010).
[11] A. van Staa, J. Wulfhorst, A. Vogel, U. Merkt, and G. Meier, Phys. Rev. B **77**, 214416 (2008).
[12] A. Vogel, J. Wulfhorst, and G. Meier, Applied Physics Letters **94**, 122510 (2009).
[13] F. J. Jedema, A. T. Filip, and B. J. van Wees, Nature **410**, 345 (2001).
[14] G. Meier, M. Bolte, R. Eiselt, B. Krüger, D.-H. Kim, and P. Fischer, Phys. Rev. Lett. **98**, 187202 (2007).
[15] G. Nahrwold, L. Bocklage, J. M. Scholtyssek, T. Matsuyama, B. Krüger, U. Merkt, and G. Meier, Journal of Applied Physics **105** (2009), http://dx.doi.org/10.1063/1.3062828.
[16] G. Nahrwold, J. M. Scholtyssek, S. Motl-Ziegler, O. Albrecht, U. Merkt, and G. Meier, Journal of Applied Physics **108** (2010).
[17] FlipseJ., B. L., SlachterA., D. K., and van WeesB. J., Nat Nano **7**, 166 (2012).
[18] K. Uchida, S. Takahashi, K. Harii, J. Ieda, W. Koshibae, K. Ando, S. Maekawa, and E. Saitoh, Nature **455**, 778 (2008).
[19] K. Uchida, T. Ota, H. Adachi, J. Xiao, T. Nonaka, Y. Kajiwara, G. E. W. Bauer, S. Maekawa, and E. Saitoh, Journal of Applied Physics **111**, 103903 (2012).
[20] H. Adachi, K. Uchida, E. Saitoh, and S. Maekawa, Reports on Progress in Physics **76**, 036501 (2013).
[21] A. Tulapurkar and Y. Suzuki, Solid State Communications **150**, 466 (2010), spin Caloritronics.
[22] R. D. Barnard, *Thermoelectricity in Metals and Alloys* (Taylor and Francis Ltd, 1972).
[23] M. Johnson and R. H. Silsbee, Phys. Rev. B **35**, 4959 (1987).
[24] E. Saitoh, G. E. W. Bauer, and B. J. van Wees, Nature Materials **11**, 391 (2012).
[25] S. R. Boona, R. C. Myers, and J. P. Heremans, Energy Environ. Sci. **7**, 885 (2014).
[26] C. M. Jaworski, J. Yang, S. Mack, D. D. Awschalom, R. C. Myers, and J. P. Heremans, Phys. Rev. Lett. **106**, 186601 (2011).
[27] J. Xiao, G. Bauer, K. Uchida, E. Saitoh, and S. Maekawa, Phys. Rev. B **81**, 214418 (2010).
[28] K. Uchida, H. Adachi, T. Ota, H. Nakayama, S. Maekawa, and E. Saitoh, Applied Physics Letters **97** (2010).
[29] K. Uchida, H. Adachi, T. Ota, H. Nakayama, S. Maekawa, and E. Saitoh, Applied Physics Letters **97**, 172505 (2010).
[30] M. Di Gennaro, A. Miranda, T. Ostler, A. Romero, and M. Verstraete, in preparation (2016).
[31] C. M. Jaworski, J. Yang, S. Mack, D. D. Awschalom, J. P. Heremans, and R. C. Myers, Nat Mater **9**, 898 (2010).
[32] Y. Kajiwara, K. Harii, S. Takahashi, J. Ohe, K. Uchida, M. Mizuguchi, H. Umezawa, H. Kawai, K. Ando, K. Takanashi, S. Maekawa, and E. Saitoh, Nature **464**, 262 (2010).
[33] J. M. Ziman, *Electrons and phonons: the theory of transport phenomena in solids*, International series of monographs on physics (Clarendon Press, Oxford, 1960).
[34] P. B. Allen, Phys. Rev. B **17**, 3725 (1978).
[35] M. Lundstrom, *Foundamentals of carrier transport* (Cambridge University Press, 1990).
[36] F. Bloch, Zeitschrift f ur Physik **52**, 555 (1929).
[37] F. Bloch, Zeitschrift für Physik **59**, 208 (1930).
[38] E. Grüneisen, Ann. Phys. (Leipzig) **4**, 530 (1933).
[39] H. Diep, Y. Magnin, and D. Hoang, Proceedings of the European Conference Physics of Magnetism **121** (2012).
[40] K. Behnia, *Fundamentals of Thermoelectricity* (Oxford University Press, 2015).
[41] B. Xu and M. J. Verstraete, Phys. Rev. Lett. **112**, 196603 (2014).
[42] E. Villamor, M. Isasa, L. E. Hueso, and F. Casanova, Phys. Rev. B **88**, 184411 (2013).
[43] G. K. Madsen and D. J. Singh, Computer Physics Communications **175**, 67 (2006).
[44] K.-H. Hellwege and J. O. (Eds.), *Electrical Resistivity, Thermoelectrical Power and Optical Properties*, Vol. 15b (Springer Berlin Heidelberg, 1985).
[45] M. Zhu, C. L. Dennis, and R. D. McMichael, Phys. Rev. B **81**, 140407 (2010).
[46] F. J. Blatt, D. J. Flood, V. Rowe, P. A. Schroeder, and J. E. Cox, Phys. Rev. Lett. **18**, 395 (1967).
[47] A. Fert and I. A. Campbell, Journal of Physics F: Metal Physics **6**, 849 (1976).